

Detailed 3D Simulation of the GEM-based detector

This content has been downloaded from IOPscience. Please scroll down to see the full text.

2016 J. Phys.: Conf. Ser. 759 012071

(<http://iopscience.iop.org/1742-6596/759/1/012071>)

View [the table of contents for this issue](#), or go to the [journal homepage](#) for more

Download details:

IP Address: 14.139.217.114

This content was downloaded on 10/05/2017 at 04:26

Please note that [terms and conditions apply](#).

You may also be interested in:

[Recent developments in GEM-based neutron detectors](#)

K Saenboonruang

[A GEM-based thermal neutron detector for high counting rate applications](#)

E. Perelli Cippo, G. Croci, A. Muraro et al.

[Advances in ion back-flow reduction in cascaded gaseous electron multipliers incorporating R-MHSP elements](#)

A V Lyashenko, A Breskin, R Chechik et al.

[Development of GEM-based Read-Out Chambers for the upgrade of the ALICE TPC](#)

P Gasik

[Comparison of Experiment and Simulation of the triple GEM-Based Fast Neutron Detector](#)

Wang Xiao-Dong, Zhang Jun-Wei, Hu Bi-Tao et al.

[Neutron beam imaging with GEM detectors](#)

G. Albani, G. Croci, C. Cazzaniga et al.

[Application of GEM-based detectors in full-field XRF imaging](#)

W. Dbrowski, T. Fiutowski, P. Frczek et al.

[Decoupling in the problem of tokamak plasma response to asymmetric magnetic perturbations](#)

V D Pustovitov

[Diffraction measurements with a boron-based GEM neutron detector](#)

Gabriele Croci, Giorgia Albani, Carlo Cazzaniga et al.

Detailed 3D Simulation of the GEM-based detector

P Bhattacharya¹, S Biswas², B Mohanty¹, N Majumdar³ and S Mukhopadhyay³

¹ School of Physical Science, National Institute of Science Education and Research, Jatni, Khurda, Odisha, India 752050

² Physics Department, Bose Institute, Block - EN, Saltlake, Kolkata, India 700091

³ Applied Nuclear Physics Department, Saha Institute of Nuclear Physics, 1/AF, Bidhannagar, Kolkata, India 700064

E-mail: purba.bhattacharya85@gmail.com

Abstract. The operation of Micro Pattern Gaseous Detectors (MPGDs) has often suffered from effects such as distortion of the electric field due to space charge, despite their widespread use in particle-physics and nuclear-physics experiments, astro-particle research, medical imaging, material science etc. To keep distortions due to space-charge at a manageable level, a lower ion feedback is required while maintaining substantial detector gain and good resolution. Thus, a proper optimization of the detector geometry, field configuration and gas mixtures are required to have a higher electron transparency and lower ion backflow. In our work, Garfield simulation framework has been adopted as a tool to evaluate the fundamental features of Gas Electron Multiplier (GEM). Our study begins with the computation of electrostatic field and its variation with different geometrical and electrical parameters using the neBEM toolkit. Different efficient algorithms have been implemented to increase the computational efficiency of the field solver. Finally, ion backflow and electron transparency of single and quadruple GEMs with different geometry and field configurations suitable for the ALICE-TPC, have been studied.

1. Introduction

ALICE at the LHC is planning a major upgrade of its detector systems, including the main tracking device, Time Projection Chamber, to cope with an increase of the LHC luminosity after 2018 [1]. This implies replacement of the present Multi Wire Proportional Counter (MWPC) based readout system of the TPC by continuously operated amplification scheme. The Micro-Pattern Gaseous Detectors (MPGDs) [2] are among the possible options as tracking and triggering detectors in highly luminous environments. The ALICE-TPC collaboration are currently working on the adoption of the Gas Electron Multiplier (GEM) [3] as the readout system of the TPC [4]. The new readout chambers will employ stacks of four GEM foils for gas amplification and anode pad readout. However, several questions related to the operation of the GEM have to be answered before it can be finally chosen as the possible solution. The major challenge is to have a low ion feedback in the drift volume to keep distortions due to space-charge at a manageable level [5]. At the same time, to retain the specific energy loss for a good particle identification, the fraction of primary electrons that participate in the avalanche process, should be large. With a proper optimization of the detector geometry, field configuration and gas mixtures, a high electron transparency, as well as, low ion backflow can be obtained.



Keeping the requirement in mind, in the present work, the electron transparency and ion backflow fractions of GEM-based detectors have been numerically estimated. We initiated with the computation of electrostatic field and its variation with different geometrical and electrical parameters. Parallel processing and other efficient algorithms have been implemented to increase the computational efficiency of the field solver. Detailed studies have been carried out in order to optimize various aspects of the simulation framework so that complex physics problems can be approached keeping the demand of computational resources at an acceptable level. The effects of detector geometry, electric and magnetic field on electron transparency and ion backflow fraction have been carried out extensively. To begin with, single GEM configurations have been studied in detail. A good understanding of the complex physics process in this device has allowed us to deal with relative ease the quadruple GEM configurations, which is being considered as a possible option for the ALICE TPC. In this manner, it has been possible for us to achieve a understanding of the likely optimum configurations of the quadruple GEMs.

2. Simulation Tools

Garfield [6] simulation framework which provides interface to other software packages, such as neBEM (nearly exact Boundary Element Method) [7], HEED [8] and Magboltz [9], has been used for the present work. neBEM is the toolkit to compute 3D electrostatic field whereas, HEED has been used for primary ionization calculation and Magboltz for computing electron and ion transport properties in gas.

3. Numerical Models

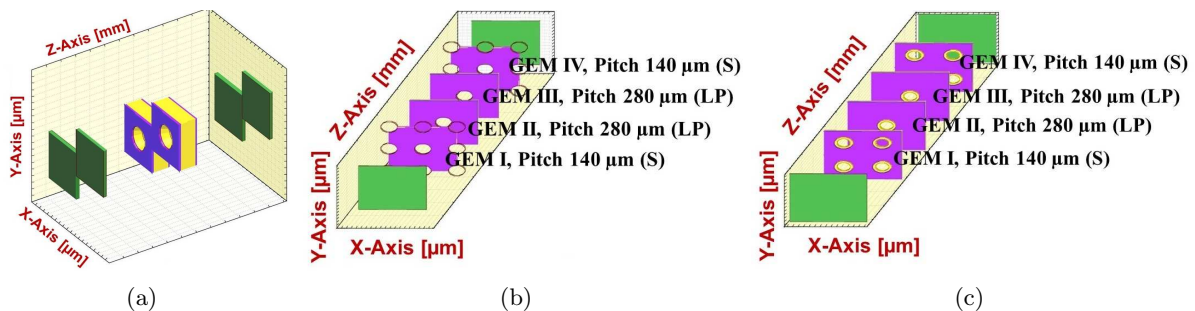


Figure 1: Model for (a) single and quadruple GEM with (b) aligned and (c) misaligned holes

The geometrical parameters of GEM-based detectors, used in the numerical work, are listed in table 1. The model of a basic GEM cell built using Garfield, is shown in figure 1(a). It represents a GEM foil, having two bi-conical shaped holes placed in a staggered manner along with a readout anode and a drift plane on either sides of the foil. The distance between top surface of the GEM and the drift plane is called the drift gap whereas that between the lower surface and the readout plate is named induction gap. In comparison to single GEM, in case of multi GEM detector, several GEM foils are placed in between the drift and the read-out plane. The naming scheme used in this work, numbers the foils in the increasing order towards the anode plate. The top most GEM is called GEM I and the others are GEM II, GEM III and so on. The gap in between GEM I and II is called transfer gap I and that between GEM II and III is called transfer gap II etc. For example, the simulation models of two different quadruple GEM devices are shown in figure 1. Among the four foils, GEM I and GEM IV, have the pitch of $140 \mu\text{m}$ (denoted as S), whereas the middle two foils have a larger pitch of $280 \mu\text{m}$ (denoted as LP). This arrangement, denoted S-LP-LP-S, employs asymmetric transfer fields and foils with low optical transparency and, thus, allows to block ions efficiently. Two different geometrical

variation in case of four GEM foils have been considered. In the first case (QGEM I), the central hole of the basic unit from all the four GEM foils are perfectly aligned (figure 1(b)). In the other case (QGEM II), as shown in figure 1(c), the first and the last foils (S) are aligned with each other whereas the second and third foils (LP) are misaligned with them. The basic cell structure then has been repeated along both positive and negative X and Y-Axes to build the actual dimension of the real detector. With the help of these models, the field configuration of the detectors have been simulated using appropriate voltage settings. These are followed by the simulation of electron transmission and ion backflow fraction in Ne : CO₂ : N₂ (90:10:5) gas mixture.

Table 1: GEM design parameters.

Polymer substrate	50 μm
Copper thickness	5 μm
Outer hole diameter	70 μm
Inner hole diameter	50 μm
Hole to hole pitch	140 / 280 μm
Drift Gap	3 mm
Transfer gap	2 mm
Induction gap	2 mm

Table 2: Voltage of Quadruple GEM.

Drift Field	0.4 kV/cm
ΔV_{GEMI}	275 V
Transfer Field I	4 kV/cm
ΔV_{GEMII}	235 V
Transfer Field II	2 kV/cm
ΔV_{GEMIII}	284 V
Transfer Field III	0.1 kV/cm
ΔV_{GEMIV}	345 V
Induction Field	4 kV/cm

For the calculation of electron transmission, 10,000 electrons have been injected in the drift gap in random positions. These electrons are made to drift towards the GEM foil using the Microscopic tracking routine. In this procedure, a electron drift path goes through millions of collisions such as elastic or inelastic collision, excitation, ionization, attachment etc. The electron transmission has been estimated as the ratio between the number of electrons that reach the anode plate to that created in the drift volume.

The electrons during their drift produce avalanche inside the GEM foil. The ions created during the avalanche process, as well as the primary ions, have been considered for the calculation of ion backflow. The fraction of total ions that drift back to drift volume, gives the desired estimation.

4. Results

4.1. Field Solver

A commonly accepted approach to solve electrostatic problems for arbitrary three-dimensional geometries is the Boundary Element Method (BEM). A novel formulation of the BEM, the nearly exact BEM (neBEM) solver was developed to resolve some of the major drawbacks of usual BEM. The neBEM uses exact integration of the Greens function and its derivative in its formulation. In this approach, these integrations for rectangular and triangular elements having uniform charge density have been obtained as a closed-form analytical expressions using symbolic mathematics. Thus, these foundation expressions account for truly distributed nature of charge density on a given element. The major advantage achieved through the use of the proposed closed-form expressions is that the accuracy is enhanced throughout the physical domain including near-field region without using any special formulation in any part of the domain. During the course of this work, the neBEM toolkit has been improved significantly. The major challenge in these developments has been to increase the efficiency of the solver, while maintaining its precision.

Code parallelization: Recently, we have successfully implemented Open Multi-Processing (OpenMP) for the neBEM field solver. It is an Application Programming Interface (API)

for multi-platform shared memory multiprocessor programming. We have tested these implementations on 2, 4 and 8 cores. The observed reduction in the computational time has been found to be significant while the precision of the solution has been found to be preserved. In the following table 3, we present a comparison of the time taken to solve charge densities for typical problems of single GEM detector involving 1126 number of elements and 116 repetitions of the basic structure.

Adaptive Modelling: In adaptive meshing the solution is usually attempted at a given spatial discretization and the solver is expected to increase or decrease the meshing to meet the desired accuracy specifications. For neBEM, we have presently implemented an algorithm which allows us to ignore the finer variations of charge densities on a primitive provided (i) it is not on the base device and (ii) it is at a far enough location so that the influence of the average charge density on the primitive is equivalent to the influence that is estimated preserving the real charge density variation on the primitive. The effect of using different values of primAfter on the same problem of GEM detector has been listed in table 4. In the present case, it has been noted that setting primAfter = 5 has negligible effect on the evaluated potential and field for this device.

Fast Volume: As is expected, the time to estimate potential and field for a complex device is significant. Reduction of time taken to estimate the electrostatic properties becomes increasingly important when complex processes such as Avalanche, Monte-Carlo tracking and Micro-Tracking are being modelled. In order to model these phenomena within a reasonable span of time, we have implemented the concept of using pre-computed values of potential and field at large number of nodal points in a set of suitable volumes. These volumes are chosen such that they can be repeated to represent any region of a given device and simple trilinear interpolation is used to find the properties at non-nodal points. The associated volume is named as the Fast Volume and in the table 5, in case of GEM detector, the potential and fields estimated by direct evaluation and those using FastVol have been compared.

Table 3: Effect of OMP.

Table 4: Effect of AM.

Table 5: Effect of FastVol.

Core 1	20.67 min	PrimAfter 0	1.47 min	Problem	Without	With
Core 2	11.32 min	PrimAfter 10	0.97 min	Charge density	1 min	32 min
Core 4	6.02 min	PrimAfter 5	0.60 min	Field Map	41 hr	4 min
Core 8	4.77 min	PrimAfter 2	0.58 min	Avalanche	2 days	19 sec

4.2. Electron Transmission

Electron transmission can be presented as a function of two mechanisms: electron focusing and transverse diffusion. Electron focusing depends not only on the field ratio, but also on different geometrical parameters. On the other hand, the transverse diffusion is mainly affected by the electric field and the gas composition. Besides that, the electron attachment coefficient, can also influence transmission. For a single GEM detector, the total electron transmission (ϵ_{tot}) can be identified as the multiplication of two efficiencies, the collection efficiency (ϵ_{coll}) and the extraction efficiency (ϵ_{ext}). These two efficiencies are defined as follows:

$$\epsilon_{coll} = \frac{\text{Electrons reached inside the GEM foil}}{\text{Electrons created in drift volume}}; \quad \epsilon_{ext} = \frac{\text{Electrons reached the readout plane}}{\text{Electrons present inside the GEM foil}} \quad (1)$$

The variations of ϵ_{coll} , ϵ_{ext} and ϵ_{tot} under different field configurations have been plotted in figure 2. For a fixed V_{GEM} and $E_{Induction}$, ϵ_{coll} decrease with the increase of the drift field,

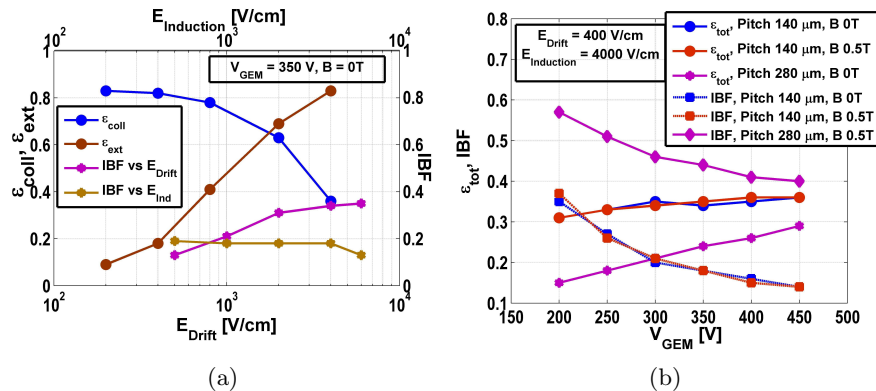


Figure 2: Variation of (a) ϵ_{coll} , ϵ_{ext} and IBF with E_{Drift} and (b) $E_{Induction}$; (b) ϵ_{tot} and IBF with V_{GEM} . Effect of pitch and magnetic field are shown in (b).

Table 6: ϵ_{coll} and ϵ_{ext} of quadruple GEMs.

Geometry	B (T)	ϵ_{collI}	ϵ_{extI}	$\epsilon_{collIII}$	ϵ_{extII}	$\epsilon_{collIII}$	ϵ_{extIII}	ϵ_{collIV}	ϵ_{extIV}
QGemI	0	0.989	0.349	0.067	0.310	0.151	0.135	0.929	0.372
QGemI	0.5	0.993	0.354	0.071	0.305	0.142	0.130	0.930	0.374
QGemII	0.5	0.893	0.391	0.069	0.313	0.175	0.128	0.928	0.360

whereas at a fixed V_{GEM} and E_{Drift} , the increase of induction field, increases ϵ_{ext} as shown in figure 2(a). The change of V_{GEM} only has effect on ϵ_{coll} and thus ϵ_{tot} (figure 2(b)). It is also seen from figure 2(b), for the same voltage configuration, the smaller pitch GEM foils is better in terms of higher electron transmission, whereas 0.5 T magnetic field plays no significant effect on it.

The voltage configuration, used for quadruple GEM detectors, are listed in table 2. For the multi-GEM detectors, the electron transmission can be also identified as the multiplication of collection and extraction efficiencies of the individual GEM foils. ϵ_{coll} and ϵ_{ext} of individual GEM foils for a quadruple GEM detectors (QGemI) have been listed in table 6. No significant effect of the magnetic field on ϵ_{tot} has been observed till now.

4.3. Ion Backflow Fraction

The backflow fraction mainly depends on the field ratio and the transverse spread of the electron avalanche. Thus, a proper optimization of the field in the drift volume, GEM hole and induction regions is necessary to prevent those ions from entering the drift volume. The ion backflow of a single GEM can be reduced by decreasing E_{Drift} (figure 2(a)) because less number of field lines will get out of the hole into the drift volume. At higher E_{Drift} , the ratio between E_{Drift} and E_{GEM} is large resulting in the drift of more number of ions into the drift volume. No significant effect of $E_{Induction}$ has been observed except at the higher $E_{Induction}$ (figure 2(a)). At higher E_{GEM} , the ratio between E_{Drift} and E_{GEM} is small and thus a large fraction of ions is collected at the top surface of the GEM foil. From figure 2(b), it is also seen that the GEM foil with standard pitch of 140 μ m gives less backflow fraction, whereas no significant effect of 0.5T magnetic field on backflow has been observed.

A better suppression of the backflow can be achieved by using multiple GEM structures. The ion collection efficiencies of four foils for the two different geometry have been listed in table 7.

Table 7: ion collection of quadruple GEM detectors.

Geometry	B (T)	GEMI	GEMII	GEMIII	GEMIV	Drift
QGEM I	0	0.025	0.004	0.013	0.932	0.027
QGEM II	0.5	0.023	0.004	0.013	0.930	0.028
QGEM II	0.5	0.059	0.005	0.012	0.923	0.001

The backflow for the first case is $\sim 2.7\%$, whereas the misaligned holes decrease its value to $\sim 0.1\%$. The effect of magnetic field has been studied in conjunction with the case when there is no magnetic field. No effect of 0.5T field on overall backflow fraction has been observed.

5. Conclusion

In the present work, the electron transmission and ion backflow fraction for different GEM-based detectors have been evaluated numerically. Several modifications have been made in the simulation framework to make it significantly efficient and, as a result, suitable to study the complex physics problems of such devices. Efficiency of the field-solver has been enhanced to a great extent. Detailed studies have been carried out in order to optimize various aspects of the simulation framework so that complex physics problems can be approached keeping the demand of computational resources at an acceptable level, without losing on the precision front. Study of single GEM detectors shows that higher electron transmission and lower backflow fraction can be obtained with higher GEM voltage, lower drift field and higher induction field. GEM foils with larger pitch gives better electron transmission, as well as less backflow fraction. Multi-GEM devices are found to be better in terms of lower backflow fraction though the electron transmission is affected adversely. Several studies on quadruple GEM detectors with various geometry and field configuration have been performed. No significant effect of 0.5T magnetic field has been observed. Further work is necessary to achieve a comprehensive understanding as well as to find out an optimal geometry and field configuration in the context of the ALICE-TPC upgrade scenario.

Acknowledgments

We thank the members of the RD51 and ALICE-TPC collaboration for their help and valuable suggestions. We also acknowledge our respective Institutions for supporting us with the necessary facilities.

References

- [1] Gasik P 2013 *J. Instrum.: Conf. Series* **9** C04035
- [2] Hoch M 2004 *Nucl. Instrum. Method A* **535** 1
- [3] Sauli F 1997 *Nucl. Instrum. Meth. A* **386** 531
- [4] ALICE Collaboration 2014 *CERN-LHCC-2015-002 /ALICE-TDR-106-ADD-1*
- [5] Ball M, Eckstein and Gunji T 2013 *J. Instrum.: Conf. Series* **9** C04025
- [6] <http://cern.ch/garfield>.
- [7] <http://cern.ch/neBEM>.
- [8] <http://cern.ch/heed>.
- [9] <http://cern.ch/magboltz>.